Robust motion control of aerial manipulators

(Article begins on next page)

Robust Motion Control of Aerial Manipulators[★]

N. Mimmo[∗], A. Macchelli, R. Naldi, L. Marconi

Department of Electrical, Electronic, and Information Engineering (DEI) "Guglielmo Marconi," University of Bologna,
viale del Risorgimento 2, 40136 Bologna, Italy.
email:{nicola.mimmo2, alessandro.macchelli, roberto.naldi, lorenzo.marconi}@unibo.it

Abstract

Aerial manipulators are composed of a robotic arm installed on an unmanned aerial vehicle and are used in several applications because of their inherent ability in performing complex tasks. In real-world applications, these systems are required to be robust against exogenous disturbances, such as wind, to guarantee the desired level of accuracy in the execution of the tasks. In this paper, the reference scenario consists of an aerial manipulator with a camera mounted on the end-effector of the robotic arm, and the goal is to track a fast-moving target. A control system architecture able to assure that the tracking error remains bounded even in the presence of external disturbances is illustrated. The proposed approach is based on the compensation of the dynamic coupling between the robotic arm and the unmanned aerial vehicle. Stability is analytically proved, and the effectiveness of the proposed control solution is shown with some simulations.

Keywords: robust control, aerial robotics, nonlinear control

1. Introduction

Aerial robots are rapidly spreading thanks to their inborn mobility and inexpensiveness which make them an attractive alternative to humans in performing tasks in harsh environments. Among the plentiful number of solutions, the aerial manipulators, constituted by the union of an Unmanned Aerial Vehicle (UAV) with a robotic arm, are drawing the attention of the scientific community. Indeed, the degrees of freedom added by the introduction of the robotic arms extend the ability of the UAVs to accomplish complex tasks such as visual maintenance, tracking of moving targets, load transfer, etc [1]. In these applications, the end-effector, which constitute the terminal part of the robotic arm, is required to follow a given time varying trajectory while the UAV keeps its position to as-

sure that the robotic arm remains in its working space. The tracking performance of both the end-effector and the UAV should be guaranteed with a prescribed level of accuracy and despite the presence of unknown environmental disturbances such as the wind.

In this operative scenario, the design of control systems for aerial manipulators faces the challenging problems of the robust stabilisation and tracking of a reference trajectory in presence of disturbances [2]. These problems are worsen by the inherent under-actuated nature of most of the UAVs (e.g., multi-rotors with fixed uniaxial propellers configuration) that couples the rotational and translational dynamics, with the latter that are also subject to kinematic and dynamical constraints enforced by the aerial manipulators [3]. The under-actuated nature of the platform is necessarily handled by considering the attitude as virtual input for the position control. By governing the attitude, in fact, the thrust of the vehicle is projected along desired directions by thus indirectly controlling the position dynamics. The choice of this virtual control input requires

the ability to track the desired attitude to guarantee the stability of the whole system. In this respect any joint torque which accelerates the robotic arm results in a force-torque wrench that must be balanced by the UAV.

As for the stabilisation of the system during trajectory tracking, the problem of the coupling between the dynamics of the manipulator and the dynamics of the UAV is typically approached in different ways. One possible way is to adopt two independent control designs, one for the manipulator [4] and one for the UAV [5], fulfilling some interconnection constraints which guarantee the stability of the whole system. A second design philosophy is based on "monolithic" controllers considering the aerial manipulators as a whole. In this class of control solutions, the back-stepping approach was used in [6, 7, 8, 9] whereas the singular perturbation theory was exploited in [10]. As for monolithic solutions, it is also worth recalling solutions using non-linear model predictive controllers in [11], task oriented control strategies in [12] and adaptive controllers in [13, 14, 15]. Finally, a feedback linearisation was designed in [16, 17].

The main contribution of this work regards the design of a control system for quadcopters equipped with a three degrees of freedom robotic arm. Inspired by [18], the proposed control design strategy relies on the robust stabilisation of the end-effector, which takes advantage of the knowledge of the UAV attitude, and on the robust stabilisation of the UAV based on a direct compensation of the dynamic effects induced by the robotic arm. The plant has been modified with respect to the one presented in [18], and this implied an improvement of the control law to avoid singularities in the definition of the total thrust of the UAV. Moreover, here robustness with respect to exogenous disturbances acting on the whole state is addressed.

The paradigm adopted in this paper for the control of the UAV is based on the stabilisation of the position-attitude dynamics by using an inner-outer loop control strategy and vector-thrust design philosophy [19]. We build the controller on the idea that the position can be governed by controlling the total thrust and by tilting the airframe to orient the thrust toward the desired direction. The adoption of the proposed overall control architecture leads to the presence of two internal loops that need to be stabilised: the first concerns the interaction between the quadcopter position and attitude, which is directly re-

sponsible for the stability of the UAV, whereas the second regards the interaction between the end-effector and the quadcopter and affects the aerial manipulator stability. With this control architecture at hand, the nested saturations proposed in [20] are adopted as control solution to provide stability and robustness with bounded control laws, both for the end-effector reference tracking control and for the UAV stabilisation. Given a sufficiently smooth end-effector reference trajectory, the resulting aerial manipulator control system is demonstrated to guarantee a desired tracking performance (maximum allowed tracking error) despite the presence of bounded exogenous disturbances.

The manuscript is organised as follows. Section 1.1 concludes the introduction by defining the notations, whereas Section 2 presents the aerial manipulator and describes its dynamics. Section 3 describes the control system architecture whose performance is tested in simulation, with the latter presented in Section 4. Finally, this paper ends with the conclusions presented in Section 5.

1.1. Notations

We let $\mathbb{R}$, $\mathbb{R}_{>0}$, and $\mathbb{R}_{\geq 0}$ denote the set of real, positive real and non-negative real numbers, respectively. With $e_i \in \mathbb{R}^3$ we denote the unitary vector along the i-th coordinate. Given $x \in \mathbb{R}^n$, $|x|$ denotes the Euclidean norm, while, for a function $f : [0, +\infty) \rightarrow \mathbb{R}^k$, $k > 0$, define $|f|_\infty = \sup_{t \in [0, +\infty)} |f(t)|$, and $|f|_a = \limsup_{t \rightarrow +\infty} |f(t)|$. Given a class C^n function s, with $n > 0$, $s^{(n)}$ denotes the n-th order derivative. Moreover, given the square matrix $J \in \mathbb{R}^{n \times n}$, the minimum and the maximum singular value of J are denoted as $\underline{\sigma}(J)$ and $\overline{\sigma}(J)$ respectively.

The notion of Input-to-State Stability (ISS) with restrictions given in [20, Appendix B] is used, and reported below for sake of completeness. Consider a nonlinear system

$$\dot{x}(t) = f(x(t), u(t)) \tag{1}$$

with state $x \in \mathbb{R}^n$, input $u \in \mathbb{R}^m$, in which $f(0, 0) = 0$ and $f(x, u)$ is locally Lipschitz on $\mathbb{R}^n \times \mathbb{R}^m$. Let X be an open subset of $\mathbb{R}^n$ containing the origin, and let U be a positive number. System (1) is said to be ISS with restriction X on the initial state $x(0)$ and restriction U on the input $u(\cdot)$ if there exist class-$\mathcal{K}$ functions γ_0 and γ_u such that, for any $x(0) \in X$ and any input $u \in \mathcal{L}_\infty^m$ satisfying $|u|_\infty \leq U$, the solution $x(t)$ satisfies

- $|x|_\infty \le \max \{\gamma_0 \left(|x(0)|\right), \ \gamma_u \left(|u|_\infty\right)\}$,

- $|x|_a \le \gamma_u \left(|u|_a\right)$.

Moreover, a *saturation function* is a mapping $\sigma : \mathbb{R}^n \to \mathbb{R}^n$ such that, for $n = 1$

- $|\sigma'(s)| = \left|\dfrac{\mathrm{d}\sigma(s)}{\mathrm{d}s}\right| \le 2$, for all s,

- $s\sigma(s) > 0$, for all $s \ne 0$, $\sigma(0) = 0$,

- $\sigma(s) = \mathrm{sign}(s)$, for $|s| \ge 1$,

- $|s| < |\sigma(s)| < 1$, for $|s| < 1$.

For $n > 1$, the properties listed above are intended to hold component-wise. Finally, the list of the symbols used in this paper is reported in Table 1.

1.2. System and problem description

An aerial manipulator is a mobile robot specifically designed to perform manipulation tasks in all those environments/situations in which the human intervention could be demanding from a safety, economic or efficiency point of view. In this work the aerial manipulator is a quadcopter equipped with a three-degrees of freedom robotic arm, (see Fig. 1). The focus is on all the applications in which the goal is to let the end-effector to track a desired trajectory in the work space while the flying base, i.e. the quadcopter, remains in a fixed position. An example can be a drone equipped with a moving camera accomplishing surveillance tasks or tracking a moving target. The contribution is a control strategy that assures robust practical tracking of the end-effector position.

2. Mathematical model

Let $\mathcal{F}(O, x_1, x_2, x_3)$ denotes the inertial reference frame, and $\mathcal{F}'(O', x_1', x_2', x_3')$ the body frame, rigidly attached to the quadcopter. The attitude of $\mathcal{F}'$ with respect to $\mathcal{F}$ is described by the rotation matrix $R(\theta) \in \mathrm{SO}(3)$, with $\theta \in \mathbb{R}^3$ a parametrisation based on the Euler angles, such as the roll, pitch and yaw angles. To compute the kinematic model of the aerial manipulator in free-flight, we denote by $p \in \mathbb{R}^3$ the inertial quadcopter position, and by $q = (q_1, q_2, q_3) \in \mathbb{R}^3$ the joint angles of the robotic arm. If the function $f_{\mathrm{kin}} : \mathbb{R}^3 \mapsto \mathbb{R}^3$ provides the position of the

parameter	description
p, p_e, q	UAV, end-effector positions and arm joint angles
$p^\star, p_e^\star$	reference UAV and end-effector positions
$\tilde{p}, \tilde{p}_e$	UAV and end-effector position errors
θ_c, θ, ω	UAV reference attitude, actual attitude and rotational speed
$f_{\mathrm{kin}}(q), J(q)$	arm direct kinematics and Jacobian
d, d_e, d_ω	external disturbances
τ_q, τ, T	control inputs
M, J_{uav}	UAV mass and inertia
m	end-effector mass
$\bar{\kappa}$ and κ	end-effector and UAV saturated feedback control law
$\bar{\lambda}_1, \bar{\lambda}_2, \bar{k}_1, \bar{k}_2, \bar{\epsilon}$	robotic arm controller parameters
$\lambda_1, \lambda_2, k_1, k_2, \epsilon$	UAV position controller parameters
$\lambda_1^\star, \lambda_2^\star, k_1^\star, k_2^\star$	saturated controls reference parameters
v_c, v_{FF}	UAV overall position control and feed-forward position control
$\underline{v}_c, \underline{v}$	UAV position control lower bounds
T_c, τ_c	UAV designed thrust and torques control laws
$\tau_{\mathrm{FF}}, \tau_{\mathrm{FB}}$	UAV designed feed-forward and feed-back control torques

Table 1: List of symbols.

end-effector in the body frame $\mathcal{F}'$, then the corresponding inertial position $p_e \in \mathbb{R}^3$ is given by

$$p_e = R(\theta)f_{\mathrm{kin}}(q) + p \tag{2}$$

The inertial velocity of the end-effector $\dot{p}_e$ is then obtained by taking the time derivative of (2) as

$$\dot{p}_e = R(\theta)S(\omega)f_{\mathrm{kin}}(q) + R(\theta)J(q)\dot{q} + \dot{p}. \tag{3}$$

In (3), $\omega \in \mathbb{R}^3$ is the angular speed of the quadcopter expressed in $\mathcal{F}'$, $S(\omega) \in \mathfrak{so}(3)$ indicates the skew symmetric matrix associated to the vector ω, and $J(q) = \frac{\partial f_{\mathrm{kin}}}{\partial q}(q)$ is the geometric Jacobian of the robotic arm.

The aerial manipulator consists of two subsystems, the quadcopter and the robotic arm, that are rigidly interconnected one with the other. This means that, if $\tau_q \in$
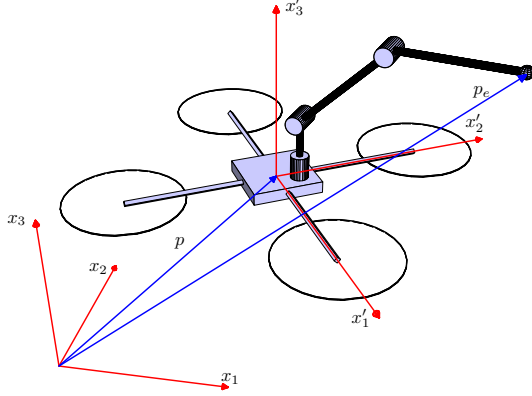
3

Figure 1: An aerial manipulator composed by a quadcopter equipped with an anthropomorphic robotic arm.

Figure 2: Graphical representation of the plant model.

$\mathcal{T}_q \subset \mathbb{R}^3$ denotes the joint torques, the internal force $R(\theta)J^{-\top}(q)\tau_q$ acts on the quadcopter and on the robotic arm in opposite directions. As a consequence, if $M > 0$ and $J_{\mathrm{uav}} \in \mathbb{R}^{3\times3}$ are the mass and the inertia tensor of the quadcopter, and if $m > 0$ is the mass of the end-effector, under the hypothesis that mass and inertia of the links of the robotic arm are negligible, the dynamic of the aerial manipulator in free-flight is

$$m\ddot{p}_e = R(\theta)J^{-\top}(q)\tau_q - mge_3 + d_e \qquad (4a)$$

$$M\ddot{p} = R(\theta)\left(Te_3 - J^{-\top}(q)\tau_q\right) - Mge_3 + d \qquad (4b)$$

$$\Omega(\theta)\dot{\theta} = \omega \qquad (4c)$$

$$J_{\mathrm{uav}}\dot{\omega} = -\omega \times J_{\mathrm{uav}}\omega - f_{\mathrm{kin}}(q) \times J^{-\top}(q)\tau_q + \tau + d_\omega \qquad (4d)$$

where $T \in [0, T_{\max}]$ is the quadcopter control thrust, $\tau \in \mathcal{T} \subset \mathbb{R}^3$ are the torques acting on the quadcopter, $\Omega : \mathbb{R}^3 \mapsto \mathbb{R}^{3\times3}$ is the matrix that maps the time derivative of the Euler's angles to the corresponding angular velocity vector ω, and the functions $d_e, d, d_\omega : \mathbb{R}_{\geq 0} \mapsto \mathbb{R}^3$ represent exogenous disturbances. The interaction between robotic arm and quadcopter dymamics is illustrated in Fig. 2. To conclude, the state of the system is $x := (p_e, p, \theta, \omega, \dot{p}_e, \dot{p}) \in X \subseteq \mathbb{R}^{18}$. We also introduce the set

$$Q := \left\{ q \in \mathbb{R}^N : \frac{\overline{\sigma}(J(q))}{\underline{\sigma}(J(q))} \leq \overline{K}_Q \right\} \qquad (5)$$

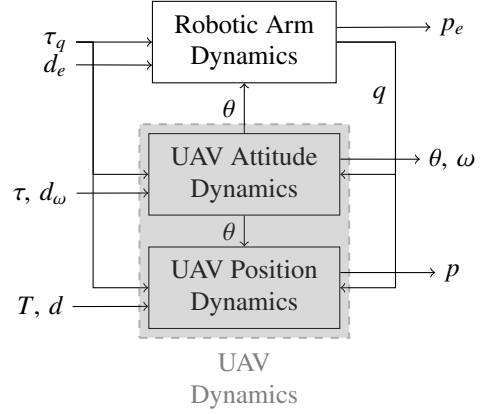that represents the set of joint variables q for which the manipulator is sufficiently far from kinematic singulari-

ties. Here, $\bar{K}_Q$ is a positive parameter. Finally, the control input is $u := (\tau_q, T, \tau) \in \mathcal{U}$, with $\mathcal{U} := \mathcal{T}_q \times [0, T_{\max}] \times \mathcal{T}$.

Remark 2.1. *The model* (4) *follows from a Lagrangian description of the aerial manipulator dynamic, in which* p, p_e *and* ω *are the Lagrangian coordinates. The inertial coupling between end-effector and UAV is taken into account by adding in the Lagrangian the virtual work that the joint torques* τ_q *do with respect to the virtual displacements associated to* p, p_e *and* θ.

3. Control design

3.1. General overview

Given the reference trajectory $p_e^\star(t)$ for the end-effector and the constant reference position $p^\star$ for the quadcopter and a desired yaw attitude $\psi^\star$, the *Aerial Manipulator Controller* is designed to robustly stabilise the system around such references. In particular as depicted in Figure 3, based on the knowledge of state of the aerial manipulator, the *Manipulator Controller* generates the joint torques τ_q to let the end-effector to robustly track $p_e^\star(t)$. At the same time, the *Quadcopter Controller*, thanks to the knowledge of τ_q, computes the thrust T and the torques τ to robustly stabilise the quadcopter in $p^\star$. As matter of fact, the overall control scheme is able to let the end-effector inertial position to track a desired reference manoeuvre, while the aerial vehicle is maintained at a constant position.
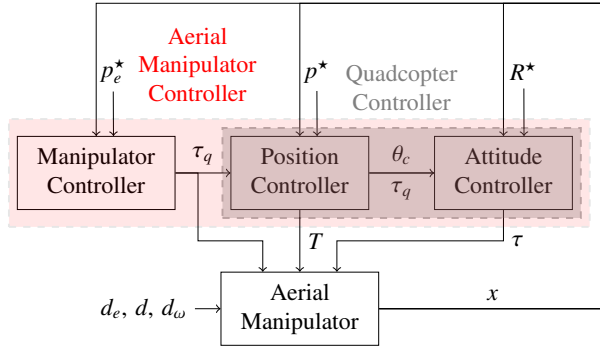
4

Figure 3: Control System Architecture

3.2. The Aerial Manipulator Controller

The coupling between the manipulator and the quadcopter takes place via the joint generalised forces τ_q and through the kinematic link (2). Manipulator and drone control systems are interlaced because, from one hand, the manipulator control action must compensate for the drone attitude and, on the other hand, the quadcopter is required to compensate for the disturbance forces introduced by the manipulator and to stabilize the desired constant lateral and vertical position.

The controller achieves asymptotic tracking of the desired references under some restrictions on the end-effector trajectory. To maintain stability, saturations are used to bound the disturbance response, i.e. the magnitude of the inputs of the manipulator and of the vehicle position controllers. In this situation, the controller achieves practical tracking of the desired references, provided that restrictions on the manipulator reference signals are taken into account. Mechanical parameters play a crucial role so as to achieve the desired stability properties. Later, in fact, it is shown the importance of keeping the mass of the manipulator sufficiently small with respect to the one of the aerial vehicle.

3.2.1. Robust control of the robotic arm

Given the reference trajectory $p_e^\star(t)$ for the inertial position of the end-effector, consider the control law

$$\tau_q = J^\top(q)R^\top(\theta)\Big[m\big(\ddot{p}_e^\star + ge_3\big) - \bar{\kappa}\big(\tilde{p}_e, \dot{\tilde{p}}_e\big)\Big] \quad (6)$$

in which $\tilde{p}_e = p_e - p_e^\star$ is the position error of the end-effector in the inertial coordinates, and where $\bar{\kappa} : \mathbb{R}^3 \times$

$\mathbb{R}^3 \to \mathbb{R}^3$ is an error feedback controller that is designed by means of the following nested saturation control law

$$\bar{\kappa}\big(\tilde{p}_e, \dot{\tilde{p}}_e\big) = \bar{\lambda}_2\sigma\left(\frac{\bar{k}_2}{\bar{\lambda}_2}\left(\dot{\tilde{p}}_e + \bar{\lambda}_1\sigma\left(\frac{\bar{k}_1}{\bar{\lambda}_1}\tilde{p}_e\right)\right)\right) \quad (7)$$

in which, by following [20, Appendix B], the parameters $\bar{k}_1, \bar{k}_2, \bar{\lambda}_1$, and $\bar{\lambda}_2$ are selected as

$$\bar{\lambda}_i = \bar{\epsilon}^{(i-1)}\lambda_i^\star \qquad\qquad \bar{k}_i = \bar{\epsilon}k_i^\star \quad (8)$$

with $i = 1, 2$, and where $k_i^\star$ and $\lambda_i^\star$ are such that

$$\frac{\lambda_2^\star}{k_2^\star} < \frac{\lambda_1^\star}{4}, \quad \frac{v_M(\bar{\epsilon})}{\bar{\epsilon}} + 4k_1^\star\lambda_1^\star < \frac{1}{m}\frac{\lambda_2^\star}{4}, \quad 6\frac{k_1^\star}{k_2^\star} < \frac{1}{24}\frac{1}{m} \quad (9)$$

with $v_M(\bar{\epsilon})$, $\bar{\epsilon} > 0$. The main properties of the manipulator (4a) driven by the control law (6)-(7) and with the system in free-flight are summarised in the next proposition, [18, Proposition 1].

Proposition 1. *Consider system* (4a) *driven by the control law (6)-(7). For all $\bar{\epsilon} > 0$, there exists $v_M(\bar{\epsilon}) > 0$ and a set of gains $\bar{k}_i$ and $\bar{\lambda}_i$, $i = 1, 2$, so that (8) and (9) hold. Then, for all initial conditions $\big(\tilde{p}_e(t_0), \dot{\tilde{p}}_e(t_0)\big) \in \mathbb{R}^3 \times \mathbb{R}^3$ and for all $d_e(t)$ such that $|d_e|_\infty \leq v_M(\bar{\epsilon})$, we have that the following holds*

- *Given $\bar{\epsilon}$ and $\lambda_2^\star$, then*

$$|\tau_q|_\infty \leq \sqrt{3}\,\overline{\sigma}(J)\Big[mg + m|\ddot{p}_e^\star|_\infty + \bar{\epsilon}\lambda_2^\star\Big] \quad (10)$$

- *There exist $\bar{\Gamma}_1, \bar{\Gamma}_2 \in \mathbb{R}_{>0}$ such that*

$$\left|\frac{\mathrm{d}\bar{\kappa}}{\mathrm{d}t}(\tilde{p}_e(t), \dot{\tilde{p}}_e(t))\right|_\infty \leq \bar{\Gamma}_1\bar{\epsilon}^2 + \bar{\Gamma}_2\bar{\epsilon}\,|d_e|_\infty \quad (11)$$

- *There exists a class-$\mathcal{KL}$ function $\beta_{\bar{\epsilon}}$ and a class-$\mathcal{K}$ $\gamma_{\bar{\epsilon}}$ such that $\forall\, t > t_0 \geq 0$*

$$|(\tilde{p}_e(t), \dot{\tilde{p}}_e(t))| \leq$$
$$\leq \gamma_{\bar{\epsilon}}\,(|d_e|_\infty) + \beta_{\bar{\epsilon}}\Big(|(\tilde{p}_e(t_0), \dot{\tilde{p}}_e(t_0))|, t - t_0\Big) \quad (12)$$

Proof. See Appendix A. □

The first item shows how the manipulator joint control actions τ_q are bounded functions, and the second one

5

shows how the first order derivative of the feedback control law can be bounded by a value that does not depend on the current tracking error and its derivatives. This bound will be taken into account later, where the interconnection between the manipulator and the aerial platform is considered. Moreover, the third item shows how the robust tracking of the desired trajectory $p_e^\star$ is achieved.

Despite the results in Proposition 1 only require the reference $p_e^\star(t)$ to be a sufficiently smooth function of time, additional constraints are introduced to support the stability results pertaining the aerial platform presented in the next subsection. The scope is to bound the influence that the manipulator has on the position and attitude dynamics of the vehicle when tracking a reference $p_e^\star$.

Assumption 3.1. *There exist three constants $\bar{D}_1^\star$, $\bar{D}_2^\star$ and $\bar{D}_3^\star \in \mathbb{R}_{>0}$ such that*

$$|\dot{p}_e^\star|_\infty \le \bar{D}_1^\star \quad |\ddot{p}_e^\star|_\infty \le \bar{D}_2^\star \quad |p_e^{\star,(3)}|_\infty \le \bar{D}_3^\star.$$

3.2.2. Position control of the quadcopter

The control design proposed in this work draws inspiration from the *thrust-vectoring* control employed to stabilize the position of under-actuated aerial configurations (see, among others, [21, 22]). The novelty of the design proposed here lies in the fact that the reaction forces applied by the manipulator back to the aerial platform are directly taken into account in the definition of the desired control force vector. To stabilise the position of aerial platform to the constant reference $p^\star$, the following *control vector* is defined

$$v_c(\tilde{p}, \dot{\tilde{p}}, t) = v_{\text{FF}}(t) - \kappa(\tilde{p}, \dot{\tilde{p}}) \quad (13)$$

in which $\tilde{p} = p - p^\star$ is the position error, $\kappa : \mathbb{R}^3 \times \mathbb{R}^3 \to \mathbb{R}^3$ is a control law and $v_{\text{FF}}(t)$ is the feed-forward term

$$v_{\text{FF}}(t) = Mge_3 + R(\theta(t))J^{-\top}(q(t))\tau_q(t). \quad (14)$$

The control vector v_c is applied to the vehicle position dynamics (4b) by properly *vectorizing* the thrust produced by the propeller. By taking advantage of the knowledge of the manipulator control inputs τ_q, a *control thrust* T_c and a *control attitude* θ_c are computed to have

$$R(\theta_c(\tilde{p}, \dot{\tilde{p}}, t))T_c e_3 = v_c(\tilde{p}, \dot{\tilde{p}}, t). \quad (15)$$

To solve (15), let us assume that, for all $t \ge 0$, there exists a positive real $\underline{v}$ such that

$$|v_{\text{FF}}(t)| \ge Mg - \frac{|\tau_q|_\infty}{\underline{\sigma}(J(q(t)))} \ge \underline{v} > 0 \quad (16)$$

and also that the feedback law $\kappa(\tilde{p}, \dot{\tilde{p}})$ is designed to guarantee that

$$|v_c(\tilde{p}, \dot{\tilde{p}})| \ge \underline{v} - |\kappa(\tilde{p}, \dot{\tilde{p}})| > \underline{v}_c \quad (17)$$

for some positive real $\underline{v}_c$. The positive lower bound $\underline{v}_c$ is necessary to avoid singular configurations for θ_c. Then, the desired thrust T_c and the desired attitude $R(\theta_c)$ that satisfy (15) are

$$T_c = |v_c(\tilde{p}, \dot{\tilde{p}})| \quad R(\theta_c(\tilde{p}, \dot{\tilde{p}}))e_3 = \frac{v_c(\tilde{p}, \dot{\tilde{p}})}{|v_c(\tilde{p}, \dot{\tilde{p}})|}. \quad (18)$$

It is worth noting that despite (18) are well defined, for all $t \ge 0$ due to (16) and (17), they only fix the first two components of θ_c. By imposing, in addition, the desired attitude $\psi^\star$, we obtain a $R^\star(t)$: $R_c(\theta_c(0, 0, t)) = R^\star(t)$ such that the yaw is $\psi^\star$. While the control thrust T_c can be directly applied to the vehicle by choosing $T = T_c$, the control attitude θ_c is employed as a reference for the attitude stabilising control law.

To stabilize the position dynamics of the aerial vehicle, we focus on the following nested saturation control law

$$\kappa\left(\tilde{p}, \dot{\tilde{p}}\right) = \lambda_2 \sigma\left(\frac{k_2}{\lambda_2}\left(\dot{\tilde{p}} + \lambda_1 \sigma\left(\frac{k_1}{\lambda_1}\tilde{p}\right)\right)\right) \quad (19)$$

in which k_1, k_2, λ_1, and λ_2 are selected as

$$\lambda_i = \epsilon^{(i-1)}\lambda_i^\star \quad k_i = \epsilon k_i^\star \quad (20)$$

with $i = 1, 2$, $\epsilon > 0$, and where $k_i^\star$, $\lambda_i^\star$ are the same of Proposition 1.

Proposition 2. *Consider the control law (19) in which k_i and λ_i, $i = 1, 2$, have been selected according to (20) and (9), with $\epsilon > 0$. Let the trajectory of the complete system be such that that $q \in Q$, with Q defined in (5) for all $t \ge 0$, the references $p_e^\star$ satisfy Assumption 3.1 and let $\epsilon > 0$ and $\bar{\epsilon} > 0$ be chosen so that*

$$Mg - \sqrt{3}\frac{\overline{\sigma}(J)}{\underline{\sigma}(J)}\left(mg + |\ddot{p}_e^\star|_\infty + \bar{\epsilon}\lambda_2^\star\right) \ge \underline{v} > \sqrt{3}\lambda_2^\star\epsilon \quad (21)$$

for some $\underline{\nu} > 0$. Furthermore, let

$$\Gamma_\eta(\theta, \theta_c, \tau_q) := [R(\theta) - R(\theta_c)] \left[T_c e_3 - J^{-\top}(q)\tau_q \right].$$

Then, for all the initial conditions $\left(\tilde{p}(t_0), \dot{\tilde{p}}(t_0) \right) \in \mathbb{R}^3 \times \mathbb{R}^3$ and for all $\theta(t)$, $\theta_c(t)$, $\tau_q(t)$ and $d(t)$ such that $\|\Gamma_\eta(\theta, \theta_c, \tau_q) + d(t)\| \le \nu_M$, the following results hold true:

- $|\kappa(\tilde{p}, \dot{\tilde{p}})|_\infty \le \sqrt{3}\lambda_2^\star \epsilon;$

- *Let the reference $p_e^\star(t)$ satisfy Assumption 3.1. Then,*

$$\left| \frac{\mathrm{d}\kappa}{\mathrm{d}t}(\tilde{p}(t), \dot{\tilde{p}}(t)) \right|_\infty \le \Gamma_{\bar{D}_2^\star} \epsilon^2 + \Gamma_2 \epsilon |d|_\infty \qquad (22)$$

  for some $\Gamma_{\bar{D}_2^\star}$, Γ_2 positive;

- *There exists a class-$\mathcal{K}_\infty$ function, γ_ϵ, such that the trajectories $(\tilde{p}, \dot{\tilde{p}})$ are asymptotically bounded by $|(\tilde{p}(t), \dot{\tilde{p}}(t))|_a \le \gamma_\epsilon(\nu_M)$.*

Proof. See Appendix B. $\qquad\qquad\square$

This result shows how the position control input is bounded by a value that does not depend on the current position error, but only on the saturation parameters. This property, together with the analogous one for the manipulator proved in Proposition 1, is used to analyse the behaviour of the overall closed-loop system in presence of disturbance preventing the vehicle to maintain the desired horizontal and vertical position asymptotically. In this context, the ISS with restriction on the inputs property is instrumental for proving the ISS stability of the complete system.

It is important to note that Propositions 1 and 2 are strictly related. In particular, to satisfy (21), the parameter $\bar{\epsilon}$ has to be selected sufficiently small. On the other hand, also the second condition in (9), that is instrumental for Proposition 1, has to hold. Consequently, $\nu_M(\bar{\epsilon})$ must be small enough. As a matter of fact, this bounds the amplitude of the disturbance $d_e(t)$ acting on the manipulator that the proposed control scheme is capable to compensate.

3.2.3. Attitude control of the quadcopter

Finally, the attitude control for the vehicle is designed. In particular, the control torque τ_c is defined as

$$\tau_c = \tau_{\mathrm{FF}}\left(\tau_q, q\right) + \tau_{\mathrm{FB}}\left(\tilde{\theta}, \dot{\theta}\right) \qquad (23)$$

in which

$$\tau_{\mathrm{FF}}\left(\tau_q, q\right) = f_{\mathrm{kin}}(q) \times \left[J^{-\top}(q)\tau_q \right] \qquad (24)$$

is the feed-forward control action compensating for the reaction torque produced by the manipulator, and

$$\tau_{\mathrm{FB}}\left(\tilde{\theta}, \dot{\theta}\right) = -k_P \left(\tilde{\theta} + k_D \dot{\theta} \right) \qquad (25)$$

is the feedback stabilising control law in which $\tilde{\theta} = \theta - \theta_c$. The stability of the overall system resulting from the interconnection with the robotic is discussed in the next proposition.

Proposition 3. *Let us consider the system* (4b)-(4d) *with state $\xi = (p, \dot{p}, \theta, \omega)$, in which the control inputs T and τ are selected as $T = T_c$ and $\tau = \tau_c$, and define the error dynamic as $\tilde{\xi}(t) = \xi(t) - (p^\star, 0, \theta_c, 0)^\top$. There exist $k_D^\star > 0$ and $\bar{\epsilon}^\star$, for all $k_D < k_D^\star$, a $k_P^\star(k_D) > 0$ such that for all $k_P > k_P^\star$ and $0 < \bar{\epsilon} < \bar{\epsilon}^\star$, there exist a $\Delta_0 > 0$, a class-$\mathcal{KL}$ function β_p and a class-$\mathcal{K}$ function γ_p such that the closed-loop system in the error coordinates $\tilde{\xi}(t)$ is ISS with restriction Δ_0 on the initial conditions and*

$$|\tilde{\xi}(t)| \le \beta_p(|\tilde{\xi}(t_0)|, t - t_0) + \gamma_p \left(|(p_e^{\star,(3)}, d_e, d, d_\omega)|_\infty \right) \quad (26)$$

for all $t \ge t_0$.

Proof. See Appendix C. $\qquad\qquad\square$

This result shows how the aerial vehicle dynamics remains bounded even in presence of the reaction forces applied by the manipulator. Hence, by considering also the result in Proposition 1 for the manipulator dynamics, the proposed control strategy achieves robust tracking of the desired references $(p^\star, p_e^\star(t))$ provided that the restrictions on the magnitude of the disturbance d_e are satisfied. Moreover, when d_e, d, $d_\omega \equiv 0$, the tracking of the manipulator references becomes asymptotic and the quadcopter converges to the desired constant position, provided that $p_e^{\star,(3)}(t) \equiv 0$, i.e. the jerk of the reference end-effector trajectory is zero.

4. Simulation results

The kinematic and dynamic models of the aerial manipulator are now simulated in Matlab with the `ode23` integrator with a maximum step size of 0.01 sec. It is

7

parameter	value
M	$1.05\,\text{kg}$
J_{uav}	$\text{diag}(0.82, 0.82, 1.64)\,\text{kg m}^2$
m	$0.1\,\text{kg}$
p'_b	$(0.1, 0.1, 0)\,\text{m}$
ℓ_1	$0.1\,\text{m}$
ℓ_2	$0.2\,\text{m}$
ℓ_3	$0.2\,\text{m}$

Table 2: Parameters of the aerial manipulator.

parameter	value
$k_1^\star$	$1\,\text{m/sec}$
$k_2^\star$	$150\,\text{kg m/sec}^2$
$\lambda_1^\star$	$5\,\text{m/sec}$
$\lambda_2^\star$	$150\,\text{kg m/sec}^2$
$\bar{\epsilon}$	0.3
ϵ	0.1
k_P	$0.05\,\text{kg m}^2/\text{sec}^2$
k_D	$40\,\text{kg m}^2/\text{sec}$

Table 3: Parameters of the controller.

Figure 4: Drone position tracking error in presence of disturbances
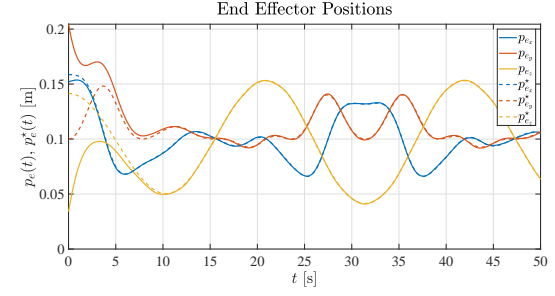
Figure 5: Actual and reference end-effector position in presence of disturbances

worth noting that, instead of adopting (4) which requires the inversion of $f_{\text{kin}}(q)$ to check if the kinematic constraints are verified, the simulator has been implemented by exploiting a Lagrangian formulation based on the direct kinematics of the robotic arm (2)-(3) and with p, θ and q as Lagrangian coordinates. The resulting model is suitable for simulation purposes because it does not require the inversion of the kinematics of the robotic arm. As far as the robot arm is concerned, an anthropomorphic configuration is adopted, with three rotational joints $q = (q_1, q_2, q_3)$. The kinematic is given by

$$f_{\text{kin}}(q) = R_3(q_1) \left[R_1(q_2) \left(R_1(q_3) e_1 \ell_3 + e_1 \ell_2 \right) + e_3 \ell_1 \right] + p'_b$$

in which $\ell_i > 0$ is the length of the i-th link, $R_j(q_i) \in$ SO(3) is the rotational matrix, around the j-th axis, associated with the rotation of the i-th joint, $i = 1, 2, 3$, and $p'_b \in \mathbb{R}^3$ is the position of the base of the manipulator in the moving frame $\mathcal{F}'$. The plant parameters are reported in Table 2, while the controller gains, selected in agreement with (8) and (20), are in Table 3.

In the operative scenario, a fast moving target that has to be tracked by the camera installed on the end-effector
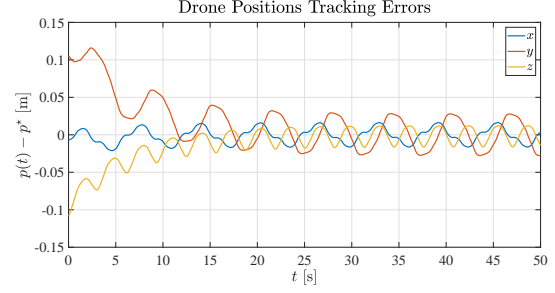
is taken into account. The initial state $x(0)$ of the aerial manipulator is randomly generated, while the end-effect reference trajectory $p_e^\star(t)$, shown in Fig. 5 (dotted lines), results from the sum of sinusoidal functions of time and simulates the required motion of the camera. The reference position of the quadcopter is for simplicity chosen as $p^\star = 0$.

The simulation has been performed in presence of exogenous disturbances which simulate a sinusoidal wind field with a time varying intensity and orientation. Such disturbances deteriorate the tracking performances of the quadcopter and of the end-effector. Since $\bar{\epsilon} > \epsilon$ and the influence of the wind on the end-effector is lower than the one on the UAV, the tracking accuracy for the end-effector position is better than the one for the drone position, see Figures 5 and 6, and Figure 4, respectively. Finally, the control actions T, τ and τ_q are depicted in Figures 7, 8 and 9, respectively.
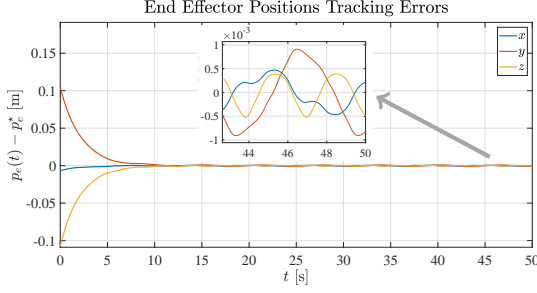
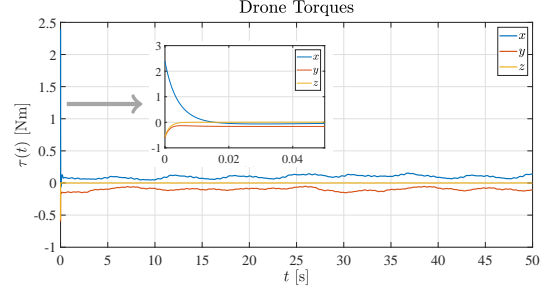Figure 6: End-effector position error in presence of disturbances
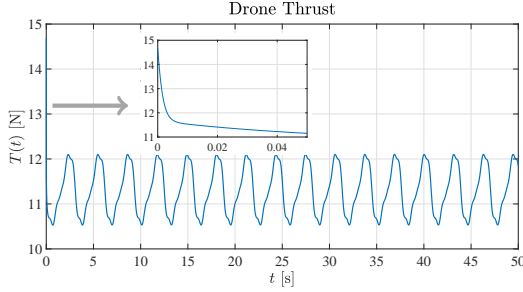

Figure 8: Drone Torques in presence of disturbances

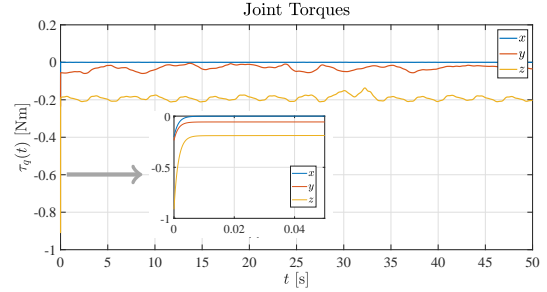Figure 7: Drone thrust in presence of disturbances

Figure 9: Joint Torques in presence of disturbances

5. Conclusions

In this paper, the design of a control system able to govern an aerial manipulator constituted of a quadcopter equipped with a three-degrees of freedom robotic arm is discussed. The robust stability of the whole system against unknown external disturbances has been achieved by means of a state-feedback controller. In particular, the robotic arm is stabilised by compensating the quadcopter attitude whereas the joint torques are directly exploited in the computation of the control law for the aerial base. The closed-loop system resulting from the interconnection of these two subsystems has been proven to be stable. Simulations demonstrate a good accuracy in case of tracking of a moving target despite the presence of exogenous disturbances.

Appendix A. Proof of Proposition 1

The first item follows from the definition of the saturation function, and from the fact that $|R(\theta)| = \sqrt{3}$. Now,

thanks to the following change of coordinates

$$\bar\zeta_1 = \tilde p_e \qquad\qquad \bar\zeta_2 = \dot{\tilde p}_e + \bar\lambda_1\sigma\left(\frac{\bar k_1}{\bar\lambda_1}\bar\zeta_1\right) \qquad (A.1)$$

the closed-loop error dynamics of the manipulator is

$$\dot{\bar\zeta}_1 = -\bar\lambda_1\sigma\left(\frac{\bar k_1}{\bar\lambda_1}\bar\zeta_1\right) + \bar\zeta_2$$

$$m\dot{\bar\zeta}_2 = -\bar\lambda_2\sigma\left(\frac{\bar k_2}{\bar\lambda_2}\bar\zeta_2\right) + m\bar k_1\sigma'\left(\frac{\bar k_1}{\bar\lambda_1}\bar\zeta_1\right)\dot{\bar\zeta}_1 + d_e(t) \qquad (A.2)$$

Note also that in the new coordinates

$$\frac{\mathrm d\bar\kappa}{\mathrm dt}(\bar\zeta_1(t),\bar\zeta_2(t)) = \frac{\bar k_2}{m}\sigma'\left(\frac{\bar k_2}{\bar\lambda_2}\bar\zeta_2\right)\cdot$$

$$\cdot\left[-\bar\lambda_2\sigma\left(\frac{\bar k_2}{\bar\lambda_2}\bar\zeta_2\right) + m\bar k_1\sigma'\left(\frac{\bar k_1}{\bar\lambda_1}\bar\zeta_1\right)\dot{\bar\zeta}_1 + d_e(t)\right] \quad (A.3)$$

By the definition of the saturation function, σ and σ' are bounded; moreover, if $|\bar{\zeta}_2| > \frac{\bar{\lambda}_2}{\bar{k}_2}$, then

$$\sigma'\left(\frac{\bar{k}_2}{\bar{\lambda}_2}\bar{\zeta}_2\right) = 0$$

and hence $\dot{\bar{\kappa}}(\tilde{p}_e(t), \dot{\tilde{p}}_e(t)) = 0$. Differently, when $|\bar{\zeta}_2| \leq \frac{\bar{\lambda}_2}{\bar{k}_2}$, from the definition of $\bar{\zeta}_1$ in (A.1) and (A.2), we have that $\dot{\bar{\zeta}}_1$ is bounded. Then, the second item of the proposition statement follows from the definition of $\bar{k}_1$, $\bar{k}_2$, $\bar{\lambda}_1$, and $\bar{\lambda}_2$ in (8) and (9). Moreover, the third item is a consequence of the fact that, as shown in [20, Appendix C], system (A.2) is ISS with non-zero restrictions (which depends on $\bar{\epsilon}$) on $d_e(t)$.

Appendix B. Proof of Proposition 2

First of all, note that (21) and $\bar{\epsilon} < \bar{\epsilon}^\star$ ensure that (16) and (17) are satisfied. The first item follows from the definition of the saturation function. To prove the second one, let us introduce the change of coordinates

$$\zeta_1 = \tilde{p} \qquad \zeta_2 = \dot{\tilde{p}} + \lambda_1 \sigma\left(\frac{k_1}{\lambda_1}\zeta_1\right). \qquad (B.1)$$

Given the position dynamics of the quadcopter (4b), and the control law (19), the position error dynamics can be written as

$$\dot{\zeta}_1 = -\lambda_1 \sigma\left(\frac{k_1}{\lambda_1}\zeta_1\right) + \zeta_2$$

$$M\dot{\zeta}_2 = -\lambda_2 \sigma\left(\frac{k_2}{\lambda_2}\zeta_2\right) + Mk_1\sigma'\left(\frac{k_1}{\lambda_2}\zeta_1\right)\dot{\zeta}_1 \qquad (B.2)$$

$$+ \Gamma_\eta(\eta_1, \tau_q) + d(t)$$

where $\Gamma_\eta(\eta_1, \tau_q)$ is the auxiliary input

$$\Gamma_\eta(\eta_1, \tau_q) = [R(\theta) - R(\theta_c)]\left[T_c\hat{e}_3' - J^{-\mathrm{T}}(q)\tau_q\right]$$

being $\eta_1 = \theta - \theta_c$ (see also Appendix C). Note that $\Gamma_\eta(0, \tau_q) = 0$ for all $\tau_q \in \mathbb{R}^3$, and for all $\eta_1 \in \mathbb{R}^3$ we have that $|\Gamma_\eta(\eta_1, \tau_q)|_\infty \leq \bar{\Gamma}_{\eta,1}|\tau_q|_\infty + \bar{\Gamma}_{\eta,2}$ for some positive constants $\Gamma_{\eta,1}$ and $\Gamma_{\eta,2}$. In the new coordinates, we have that

$$\kappa(\zeta_1, \zeta_2) = \lambda_2 \sigma\left(\frac{k_2}{\lambda_2}\zeta_2\right)$$

which implies that

$$\frac{\mathrm{d}\kappa}{\mathrm{d}t}(\zeta_1(t), \zeta_2(t)) = \frac{k_2}{M}\sigma'\left(\frac{k_2}{\lambda_2}\zeta_2\right)\left[\lambda_2\sigma\left(\frac{k_2}{\lambda_2}\zeta_2\right) + d(t)\right.$$

$$\left. + Mk_1\sigma'\left(\frac{k_1}{\lambda_1}\zeta_1\right)\dot{\zeta}_1 + \Gamma_\eta(\eta_1, \tau_q)\right]. \qquad (B.3)$$

Due to the first requirement in Assumption 3.1, namely that $|\ddot{p}_e^\star| \leq \bar{D}_2^\star$, the result is proved by considering the bound of $|\tau_q|_\infty$ given in the first item of Proposition 1, and by following the same arguments as in Appendix A. Finally, the ISS with restriction on the inputs $d(t)$, $\Gamma_\eta(\eta_1, \tau_q)$, and then τ_q and η_1, is immediate from (B.2) and the properties of the saturation functions.

Appendix C. Proof of Proposition 3

The proof is based on [18, Appendix A]. The main difference is that now we have to deal with the exogenous disturbances d and d_ω. Let us introduce the change of coordinates

$$\eta_1 = \theta - \theta_c \qquad \eta_2 = \dot{\theta} + \frac{\eta_1}{k_D}. \qquad (C.1)$$

The closed-loop attitude error dynamics can be written as

$$\dot{\eta}_1 = -\frac{\eta_1}{k_D} + \eta_2 - \dot{\theta}_c$$

$$J_{\mathrm{uav}}\Omega(\eta_1 + \theta_c)\dot{\eta}_2 = -\omega \times J_{\mathrm{uav}}\omega - k_Pk_D\eta_2 +$$

$$+ J_{\mathrm{uav}}\left[\frac{1}{k_D} + \dot{\Omega}(\eta_1 + \theta_c)\right]\cdot \qquad (C.2)$$

$$\cdot\left(\eta_2 - \frac{\eta_1}{k_D}\right) + \frac{J_{\mathrm{uav}}}{k_D}\dot{\theta}_c + d_\omega(t)$$

in which we have that

$$\omega = \Omega(\theta)\dot{\theta} = \Omega(\eta_1 + \theta_c)\left(\eta_2 - \frac{\eta_1}{k_D}\right)$$

with $\Omega(\theta)$ introduced in (4c). Note that θ_c and $\dot{\theta}_c$ are some bounded functions of R_c and $\dot{R}_c$ which, thanks to the (18), are function of v_c, $R^\star(t)$, $\dot{v}_c$ and $\dot{R}^\star(t)$. Starting from (18), the time derivative of R_c is given by

$$\dot{R}_c = \frac{v_c^\top v_c I - v_c v_c^\top}{(v_c^\top v_c)^{3/2}}\dot{v}_c$$
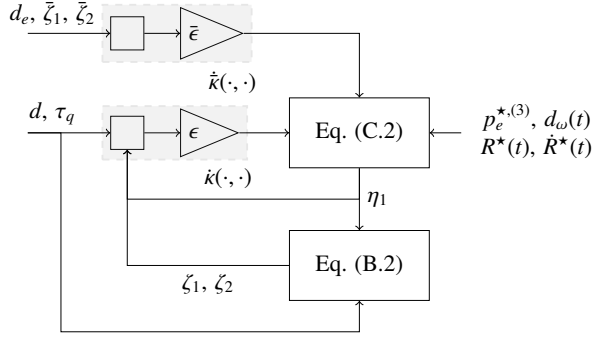
10

Figure C.10: UAV dynamics in terms of the error systems (B.2) and (C.2).

in which $(v_c^\top v_c I - v_c v_c^\top)/(v_c^\top v_c)^{3/2}$ is bounded because v_c is bounded both from below and above. Moreover, from (6) and (13) we get that

$$\dot{v}_c = m p_e^{\star,(3)} - \bar{\kappa}(\tilde{p}_e, \dot{\tilde{p}}_e) - \dot{\kappa}(\tilde{p}, \dot{\tilde{p}})$$

with $\dot{\bar{\kappa}}$ and $\dot{\kappa}$ bounded by (11) and (22), respectively.

The closed-loop dynamics of the UAV results from the feedback interconnection of (B.2) and (C.2), depicted in Fig. C.10. Due to space limitations this part of the proof is only sketched. By considering an ISS-Lyapunov function $V(\eta_1, \eta_2) = \frac{1}{2}\eta_1^\top \eta_1 + \frac{1}{2}\eta_2^\top \Omega^\top(\eta_1) J_{\text{uav}} \Omega(\eta_1)\eta_2$, and choosing k_D and k_P sufficiently small and large, respectively, and for m and $\bar{\epsilon}$ sufficiently small, system (C.2) can be shown to be ISS with respect to the exogenous input $p_e^{\star,(3)}$, $\dot{\kappa}(\tilde{p}, \dot{\tilde{p}})$, $\dot{\bar{\kappa}}(\tilde{p}_e, \dot{\tilde{p}}_e)$ and $d_\omega(t)$ with an arbitrary asymptotic gain. From Propositions 1 and 2, and from the fact that $|d_e|_\infty$, $|d|_\infty$ are bounded, it is clear that $\dot{\kappa}$ and $\dot{\bar{\kappa}}$ are also bounded. Moreover, according to Assumption 3.1, also $p_e^{\star,(3)}$ is bounded. Then, it is possible to choose k_D and k_P to satisfy the restrictions on the input (see Proposition 2) on the position error subsystem (B.2) in finite time, and then to enforce the small gain condition. The final result is a consequence of standard ISS arguments, as in [20, Appendix C].

References

[1] F. Ruggiero, V. Lippiello, A. Ollero, Aerial manipulation: A literature review, IEEE Robotics and Automation Letters 3 (2018) 1957–1964. doi:10.1109/LRA.2018.2808541.

[2] X. Meng, Y. He, J. Han, Survey on aerial manipulator: System, modeling, and control, Robotica (2019) 1–30.

[3] C. Korpela, M. Orsag, M. Pekala, P. Oh, Dynamic stability of a mobile manipulating unmanned aerial vehicle, in: 2013 IEEE International Conference on Robotics and Automation, IEEE, 2013, pp. 4922–4927.

[4] B. Siciliano, L. Sciavicco, L. Villani, G. Oriolo, Robotics: modelling, planning and control, Springer Science & Business Media, 2010.

[5] T. P. Nascimento, M. Saska, Position and attitude control of multi-rotor aerial vehicles: A survey, Annual Reviews in Control 48 (2019) 129 – 146. doi:10.1016/j.arcontrol.2019.08.004.

[6] H. Yang, D. Lee, Dynamics and control of quadrotor with robotic manipulator, in: 2014 IEEE International Conference on Robotics and Automation (ICRA), IEEE, 2014, pp. 5544–5549.

[7] G. Heredia, A. E. Jimenez-Cano, I. Sanchez, D. Llorente, V. Vega, J. Braga, J. A. Acosta, A. Ollero, Control of a multirotor outdoor aerial manipulator, in: 2014 IEEE/RSJ International Conference on Intelligent Robots and Systems, 2014, pp. 3417–3422. doi:10.1109/IROS.2014.6943038.

[8] A. E. Jimenez-Cano, J. Martin, G. Heredia, A. Ollero, R. Cano, Control of an aerial robot with multi-link arm for assembly tasks, in: 2013 IEEE International Conference on Robotics and Automation, 2013, pp. 4916–4921. doi:10.1109/ICRA.2013.6631279.

[9] S. Di Lucia, G. D. Tipaldi, W. Burgard, Attitude stabilization control of an aerial manipulator using a quaternion-based backstepping approach, in: 2015 European Conference on Mobile Robots (ECMR), 2015, pp. 1–6. doi:10.1109/ECMR.2015.7324191.

[10] M. J. Kim, K. Kondak, C. Ott, A stabilizing controller for regulation of uav with manipulator, IEEE Robotics and Automation Letters 3 (2018) 1719–1726. doi:10.1109/LRA.2018.2803205.

[11] D. Lunni, A. Santamaria-Navarro, R. Rossi, P. Rocco, L. Bascetta, J. Andrade-Cetto, Nonlinear model predictive control for aerial manipulation, in: 2017 International Conference on Unmanned Aircraft Systems (ICUAS), 2017, pp. 87–93. doi:10.1109/ICUAS.2017.7991347.

[12] A. Santamaria-Navarro, V. Lippiello, J. Andrade-Cetto, Task priority control for aerial manipulation, in: 2014 IEEE International Symposium on Safety, Security, and Rescue Robotics (2014), IEEE, 2014, pp. 1–6.

[13] S. Kim, S. Choi, H. J. Kim, Aerial manipulation using a quadrotor with a two dof robotic arm, in: 2013 IEEE/RSJ International Conference on Intelligent Robots and Systems, 2013, pp. 4990–4995. doi:10.1109/IROS.2013.6697077.

[14] E. Yilmaz, H. Zaki, M. Unel, Nonlinear adaptive control of an aerial manipulation system, in: 2019 18th European Control Conference (ECC), 2019, pp. 3916–3921. doi:10.23919/ECC.2019.8795709.

[15] M. Jafarinasab, S. Sirouspour, E. Dyer, Model-based motion control of a robotic manipulator with a flying multirotor base, IEEE/ASME Transactions on Mechatronics 24 (2019) 2328–2340. doi:10.1109/TMECH.2019.2936760.

[16] A. Y. Mersha, S. Stramigioli, R. Carloni, Exploiting the dynamics of a robotic manipulator for control of uavs, in: 2014 IEEE International Conference on Robotics and Automation (ICRA), 2014, pp. 1741–1746. doi:10.1109/ICRA.2014.6907086.

[17] L. S. Mello, G. V. Raffo, B. V. Adorno, Robust whole-body control of an unmanned aerial manipulator, in: 2016 European Control Conference (ECC), 2016, pp. 702–707. doi:10.1109/ECC.2016.7810371.

[18] R. Naldi, A. Macchelli, N. Mimmo, L. Marconi, Robust control of an aerial manipulator interacting with the environment, IFAC-PapersOnLine 51 (2018) 537 – 542. doi:10.1016/j.ifacol.2018.07.335, 2nd IFAC Conference on Modelling, Identification and Control of Nonlinear Systems MICNON 2018.

[19] R. Naldi, M. Furci, R. Sanfelice, L. Marconi, Robust global trajectory tracking for underactuated VTOL aerial vehicles using inner-outer loop control paradigms, Automatic Control, IEEE Transactions on 62 (2017) 97–112.

[20] A. Isidori, L. Marconi, A. Serrani, Robust Autonomous Guidance: An Internal Model Approach, Advances in Industrial Control, Springer–Verlag, London, 2003.

[21] M. Hua, T. Hamel, P. Morin, C. Samson, A control approach for thrust-propelled underactuated vehicles and its applications to VTOL drones, Automatic Control, IEEE Transactions on 54 (2009) 1837–1853.

[22] A. Abdessameud, A. Tayebi, Global trajectory tracking control of VTOL-UAVs without linear velocity measurements, Automatica 46 (2010) 1053–1059.